Regenerative Therapy 26 (2024) 922–931

Contents lists available at ScienceDirect

Regenerative Therapy

journal homepage: http://www.elsevier.com/locate/reth

Original Article

Spatial heterogeneity analysis of seeding of human induced pluripotent stem cells for neuroectodermal differentiation

Ali Ahmed Issa Qatan [a, 1], Shinji Tanbara [a], Masakazu Inamori [b], Kazuhiro Fukumori [a], Masahiro Kino–oka [a, b, c, *]

[a] Department of Biotechnology, Graduate School of Engineering, Osaka University, 2–1 Yamadaoka, Suita, Osaka 565–0871, Japan
[b] Cell Manufacturing Systems Engineering (Healios) Joint Research Chair, Graduate School of Engineering, Osaka University, 2–1 Yamadaoka, Suita, Osaka 565–0871, Japan
[c] Research Base for Cell Manufacturability, TechnoArena, Graduate School of Engineering, Osaka University, 2–1 Yamadaoka, Suita, Osaka 565–0871, Japan

ARTICLE INFO

Article history:
Received 10 June 2024
Received in revised form
28 September 2024
Accepted 10 October 2024

Keywords:
Spatial heterogeneity analysis
High–density cell seeding
Cell seeding operation
Human induced pluripotent stem cells
Neuroectodermal differentiation

ABSTRACT

Introduction: Preparing a uniform cell population in high–density seeding of adherent human induced pluripotent stem cells (hiPSC) requires stable culture conditions and consistent culture operation. In this study, we evaluated cell distribution patterns by changing cell seeding operations and their impact on differentiation toward the neuroectodermal lineage.
Methods: The hiPSC line 201B7 was seeded at 1.23×10^5 cells/cm^2 following a conventional operation, prolongated time of cell seeding suspension or vessel tilting during cell seeding operation. Fluorescent imaging of cell nuclei was performed 24 h following cell seeding and used for spatial heterogeneity analysis. Flow cytometric analysis was also performed seven days after cell differentiation induction toward neuroectodermal lineage.
Results: Indices for spatial heterogeneity following high–density cell seeding were proposed to assess cell distribution patterns. Global heterogeneity (H_G) was shown to be mostly affected by vessel tilting during cell seeding operation, while local heterogeneity (H_L) was affected by prolongated time of cell seeding suspension. Changes in both spatial heterogeneities in the hiPSC population resulted in a lower yield of target neuroectodermal cells compared with the control operation.
Conclusion: High–density hiPSC seeding is critical for achieving a higher yield of target cells of neuroectodermal lineage. Understanding the spatial heterogeneity in early stages detects errors in cell culture motion and predicts cell fate in later stages of cell culture.

1. Introduction

In recent years, there has been growing interest in human induced pluripotent stem cells (hiPSC) as a potentially effective resource across various research fields, including regenerative medicine, drug development, and tissue and organ modeling [1]. However, achieving effective cell manufacturability [2,3] requires overcoming challenges in stem cell manufacturing processes. To enhance cell production, it is crucial to develop innovative analytical methods that improve the consistency and efficiency of the relevant procedures. This improvement must account for the distinct characteristics of cell products, such as the natural variability within cell populations and the impact of external disturbances on the final product's quality [2,4]. Challenges include the complexity and integrity of the bioproduct, the development of a unique bioprocessing model, scaling and consistency, economic factors, and leveraging established technologies as a foundation [5].

Different patterns of spatial heterogeneity can be generated by varying certain parameters of cell seeding. The effect of selected patterns was investigated on cell fate during hiPSC differentiation toward the neuroectoderm lineage. Successful development of cell

Abbreviations: CK18, cytokeratin 18; hiPSC, human induced pluripotent stem cells; PAX6, paired box protein 6; PBS, phosphate–buffered saline; ROCK, Rho–associated kinase.

* Corresponding author. Cell Manufacturing Systems Engineering (Healios) Joint Research Chair, Graduate School of Engineering, Osaka University, 2–1 Yamadaoka, Suita, Osaka 565–0871, Japan.
E-mail address: kino-oka@bio.eng.osaka-u.ac.jp (M. Kino–oka).

Peer review under responsibility of the Japanese Society for Regenerative Medicine.

[1] This work is the basis for the Ph.D. dissertation of Ali Ahmed Issa Qatan.

https://doi.org/10.1016/j.reth.2024.10.006

Nomenclature

Parameters

A_{cell}	Area of single cell, [cm^2]
A_{nuc}	Projected area of cell nucleus, [cm^2]
A_{loc}	Local area, [cm^2]
A_{reg}	Regional area, [cm^2]
A_{global}	Global area, [cm^2]
A_{vessel}	Total area of culture vessel, [cm^2]
r_{loc}	Radius of the local area, [cm]
l_{img}	Length of sample image, [cm]
l_{reg}	Length of regional area, [cm]
r_{vessel}	Radius of the culture vessel, [cm]
n_{cell}	Cell count, [cells]
D	Distance between cell tracking points, [μm]
MSD	Mean square displacement, [μm^2]
D_{mig}	Distance of cell migration, as square root of *MSD*, [μm]
D_{enc}	Initial distance between encountering cells, [μm]

Indices

X_{loc}	Local cell density, [cells/cm^2]
X_{reg}	Regional cell density, [cells/cm^2]
$\overline{X}$	Mean local cell densities ($X_{loc,i}$) in global area, [cells/cm^2]
H_L	Local heterogeneity, [−]
H_G	Global heterogeneity, [−]

culture systems relies on a thorough understanding of cellular behavior and how it is influenced by various culture processes. An important step in this process is cell seeding into the culture vessel. Cell seeding, where cell suspension is transferred into a culture vessel or bioreactor, is crucial in achieving the desired cell distribution. Common cell culture methods often fail to distribute cells uniformly across the culture area, leading to cell aggregation around the periphery, center, or both [6]. Cell density is believed to depend primarily on the area–to–perimeter ratio rather than the size or shape of micropatterned islands [7]. By carefully examining and managing the seeding process, the desired quality of cell culture can be achieved.

Spatial heterogeneity of particle distribution is widely considered a critical measure in quality control across various manufacturing processes, as a more uniform distribution is often associated with better quality [8]. In the context of hiPSC production systems, the impact of spatial heterogeneity in cell populations remains to be thoroughly studied. Multiple approaches assess heterogeneity through the quantitative determination of key adherent cell culture characteristics, such as confluency, morphology, and cell density [7,9,10]. A non–intrusive analytical technique that allows for rapid, accurate identification and ongoing observation of the properties of adherent cultures would be highly advantageous in fields like stem cell bioprocessing and drug discovery [9,11].

We propose a method to analyze spatial heterogeneity following the cell seeding operation. We believe that the fate of a cell is closely linked to the initial conditions of the culture, including seeding density and the distribution of cells within the vessel. Studies of stem cells have shown that cell state and fate are highly regulated by cell density [12,13], where increased localized cell density can inhibit cell–cell contact [14]. Variations in cell density significantly influence cell behavior through mechanisms such as cell–cell communication, cell–substrate attachment, cell morphology, and mechanical and chemical interactions within the cell environment.

2. Materials and methods

2.1. Cells and culture conditions

The human iPSC line 201B7 was obtained from RIKEN Bioresource Center (Tsukuba, Japan), routinely maintained in an undifferentiated state on polystyrene substrate (90–mm Petri dish, Sumitomo Bakelite Co., Ltd., Shinagawa, Tokyo, Japan) coated with recombinant laminin–511 E8 fragments (0.5 μg/cm^2; iMatrix, Nippi Inc., Tokyo, Japan) in commercially available medium (StemFit AK02 N, Ajinomoto Co., Inc., Tokyo, Japan). The medium was replaced daily, and cells were incubated at 37 °C in a humidified atmosphere of 5 % CO_2. Upon reaching semi–confluence, a subculture was conducted. Cells were treated with 5 mM ethylenediaminetetraacetic acid (Nacalai Tesque, Inc., Kyoto, Japan) in phosphate–buffered saline (PBS, Thermo Fisher Scientific Inc., Waltham, MA, USA) containing 10 μM Rho–associated kinase (ROCK) inhibitor Y–27632 (CultureSure, FUJIFILM Wako Pure Chemical Corporation, Osaka, Japan) for 10 min at 37 °C. It was followed by incubation with a dissociation reagent (TrypLE Select™; Thermo Fisher Scientific Inc.) containing 10 μM ROCK inhibitor for 7 min at room temperature. Cells were collected from the culture vessel, centrifuged at 180 G for 3 min, and resuspended in a fresh culture medium. An automated cell count was performed, and the appropriate seeding volume was transferred into a new culture vessel coated with iMatrix–511.

Cell culture is divided into three phases (Fig. S1, Supplementary material): maintenance culture, expansion culture, and differentiation induction. In maintenance culture, cells were thawed, seeded at 1.0×10^4 cells/cm^2, and cultured for four days with daily medium change. Two passages of maintenance culture were conducted. In expansion, cells were seeded at 1.45×10^3 cells/cm^2 into multiple culture vessels and cultured for eight days, with medium change on days 1, 3, 5, and 7. In differentiation induction, cells were seeded at 1.23×10^5 cells/cm^2 and cultured for seven days with daily medium change. Alternations of the cell seeding operation were applied to generate different patterns of cell distributions. Before seeding into the culture vessel, the cell seeding suspension solution was maintained for 60 min, allowing cells in the bottom of the centrifuge tube and causing cell agglomeration. This method will be referred to as “waiting”. Another alternation was done by tilting the culture vessel containing the cell seeding suspension for 5 min using a tilting stand, allowing cells to settle in the culture surface unevenly. This method will be referred to as “tilting”. The medium was replaced with a differentiation induction medium (Glasgow's Minimum Essential Medium, Sigma–Aldrich, Inc., St. Louis, MO, USA) containing knockout serum replacement (20 % KSR day 1–4, 15 % KSR 5–6, Thermo Fisher Scientific Inc.), MEM non–essential amino acids solution (Thermo. Fisher Scientific Inc.), sodium pyruvate solution (Sigma–Aldrich), StemSure 2–mercaptoethanol solution (FUJIFILM Wako Pure Chemical Corporation), L–glutamine (Sigma–Aldrich), and penicillin–streptomycin (Thermo Fisher Scientific Inc.) [15]. The medium was supplemented with 10 μM ROCK inhibitor, 3 μM casein kinase 1 inhibitor (CKI–7 dihydrochloride, Sigma–Aldrich), and 5 μM type I transforming growth factor–β receptor inhibitor (SB431542, Sigma–Aldrich) throughout differentiation induction.

Cell cryopreservation was performed on day 7 of the differentiation induction. Cells were washed with PBS and treated with trypsin/ethylenediaminetetraacetic acid (FUJIFILM Wako Pure Chemical Corporation) containing 10 μM ROCK inhibitor for 10 min at 37 °C. The medium was added, and cells were collected from the

culture vessel, centrifuged at 180 G for 3 min, and resuspended in a fresh culture medium. Automated cell count was performed, and 3.0×10^6 cells/vial were dispensed into cryovials in a cryoprotectant solution (STEM–CELLBANKER GMP grade, Nippon Zenyaku Kogyo Co., Ltd., Fukushima, Japan) containing 10 μM ROCK inhibitor and stored at −80 °C.

2.2. Cell nuclei fluorescence staining

Cells were washed with PBS and fixed with 4 % paraformaldehyde (FUJIFILM Wako Pure Chemical Corporation) for 10 min at room temperature. Cells were then incubated with 0.5 % Triton X−100 in PBS for 5 min at room temperature and washed twice with Hank's balanced salt solution (Thermo Fisher Scientific Inc.). For nuclei detection, cell nuclei were stained with nucleic acid stain (167 nM, SYTOX Green Nucleic Acid, Thermo Fisher Scientific Inc.) incubated for 30 min at room temperature, washed twice, and maintained in Hank's balanced salt solution. Cells were observed under a cell imaging system (BioStation CT, Nikon Corporation, Japan) with a 4 × objective at 25 sample positions for spatial heterogeneity analysis.

2.3. Flow cytometric analysis

Suspended cells in a cryopreservation solution were thawed in a culture medium, washed with PBS, and fixed with 4 % paraformaldehyde for 10 min at 4 °C. Cells were rewashed with PBS and passed through a cell strainer to remove clumped cells, and 5.0×10^5 cells were collected. Cells were permeabilized in a fixation and permeabilization solution for 30 min at 4 °C and washed in wash buffer. Cells were stained with PE mouse anti–human PAX6 (1:200 dilution; 561552, BD Biosciences, San Jose, CA, USA), compared to isotype control PE mouse IgG2a,K Isotope (1:200 dilution; 558595, BD Biosciences), incubated for 60 min at 4 °C, and washed in wash buffer. For double staining, cells were stained with Alexa Fluor® 647 Anti–Cytokeratin 18 (1:200 dilution; 206269, Abcam, Cambridge, UK), compared to isotype control Alexa Fluor® 647 Rabbit IgG, monoclonal (1:200 dilution; 199093, Abcam), incubated for 60 min at 4 °C and washed in wash buffer. Stained cells were resuspended in 2 % fetal bovine serum in PBS, and the fluorescent intensity was detected using a flow cytometry system (CyFlow Cube 6; Sysmex Co., Kobe, Japan).

2.4. Spatial heterogeneity analysis

2.4.1. Scales of cell environment

The scale of the cell culture environment is categorized into four areas: single–cell, local, regional, and global areas (Fig. 1). Single–cell area (A_{cell}) is the projected area of a single cell, while only the centroid position of single cells is used in the current analysis method. The local area (A_{loc}) is the area where relative cell behaviors occur. These behaviors include cell movement, encounters with neighbor cells, and cell–cell contact. The regional area (A_{reg}) is the area where local heterogeneities of cell behavior are expressed and where larger subpopulations of neighboring cells might have similar conditions within the cell culture. The global area (A_{global}) is the area where global heterogeneity of cell behavior is expressed. A_{global} is the summation of A_{reg}, a representative sample of the whole culture vessel area (A_{vessel}), including the total cell population that is connected and shares the same environment and culture conditions.

2.4.2. Setting the size of the local area

The size of the local area (A_{loc}) was calculated from the cell's initial position, elongation–driven cell encounter, and cell migration–driven cell encounters following cell seeding. Cells were subcultured from maintenance cell culture to polystyrene substrates (6–well plate, Sumitomo Bakelite Co., Ltd.) at a viable cell density of 1.0×10^3 cell/cm^2 and tracked by time–lapse observations previously mentioned. The distance between track points (D) was calculated as the hypotenuse between the centroid position for the cell nucleus at the time (t) and at the next time point ($t + \Delta t$), as given in Eq. (1).

$$D_{(X_t,\ Y_t\ )} = \sqrt{(X_t - X_{t+\Delta t})^2 + (Y_t - Y_{t+\Delta t})^2} \tag{1}$$

Where $D_{(X_t,\ Y_t\ )}$ is the length of track at time t, X_t, Y_t, $X_{t\ +\ \Delta t}$, $X_{t\ +\ \Delta t}$, and $Y_{t\ +\ \Delta}$ are the centroid coordinates at t and $t + \Delta t$. The mean square displacement (MSD) and distance of cell migration (D_{mig}) were measured, as given in Eq. (2) and (3).

$$MSD = \frac{1}{N}\sum_{t=1}^{N} |D_t|^2 \tag{2}$$

$$D_{mig} = \sqrt{MSD} \tag{3}$$

Elongation–driven cell encounters were investigated 24 h after cell seeding, and cell formed elongation–driven cell encounters were selected. Retrospective tracking of the same cells was conducted, and initial cell position and distance between cell centroids (D_{enc}) were measured as given in Eq. (4).

$$D_{enc} = \sqrt{(X_a - X_b)^2 + (\ Y_a -\ Y_b)^2} \tag{4}$$

Herein, D_{enc} is the distance between the encountering cells' initial positions, X_a, Y_a, X_b, and Y_b, are the coordinates of the encountering cells' initial positions. Data of the D_{mig} of cell migration and D_{enc} are collected from 30 cells or pairs of encountering cells, where the average is calculated. Whether cells expressing higher migration or elongation–driven cell encounter, the larger value of D_{mig} or D_{enc} is set as the radius of the local area (r_{loc}). Using r_{loc}, local cell density (X_{loc}) is calculated from cell count (n_{cell}) within each local area (A_{loc}), as given in Eq. (5).

$$X_{loc} = \frac{n_{cell}}{A_{loc}} \tag{5}$$

2.4.3. Setting the size of the regional area

The size of the regional area (A_{reg}) is designed to encompass local and global heterogeneities, allowing for the possibility that larger groups of adjacent cells may experience similar conditions. A_{reg} corresponds to the region of interest extracted from a sample image (A_{img}), with A_{img} being 0.04 cm^2 captured with a 4 × magnification lens. In estimating local cell densities (X_{loc}) using the kernel analysis method, some local regions (A_{loc}) might be under–represented as they extend beyond the A_{img} boundaries. Therefore, cell counts (n_{cell}) are only recorded within sections of A_{loc} that fall within A_{img}. To ensure data integrity, the periphery of the image is trimmed to discard any partial data. The image margin is specifically trimmed by the depth of a local area's radius (r_{loc}), where A_{img} is calculated using l_{img}, the length of one side of A_{img}, as given in Eq. (6).

$$A_{reg} = (l_{img} - 2 \times r_{loc})^2 \tag{6}$$

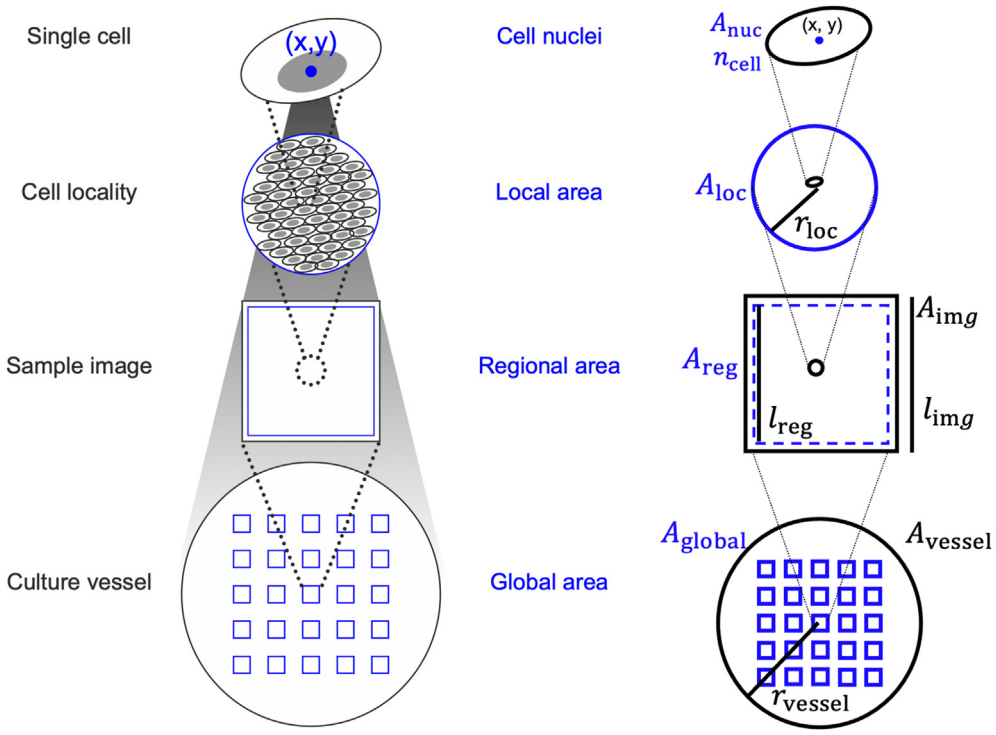

Fig. 1. Scale of Cellular Enviroment. The proposed spatial heterogeneity method considers four scales of the cellular environment: the position of cell nucleus, the local area, the regional area, and the global area, in order to represent the individual cell, the immidiate vicinity of cells, the cell population in sample image, and the entire culture vessel, respectively.

2.4.4. Setting the size of the global area

The area of the culture vessel (A_{vessel}) is defined depending on the culture vessel used, where a unit of culture vessel considers the total cell population forming a connecting cell sheet in the confluence state of a two–dimensional culture, i.e., the whole–dish area in a single–well dish or single–well area in a multiple–well plate. The 90–mm Petri dishes (A_{vessel} = 57 cm^2) used in the current study contain a large cell population, where a representative sample is required. Sample images (A_{img}) were captured at 25 positions, with a sample–population ratio of 1:57 (Fig. S2, Supplementary materials). The positions were selected to cover the central, intermediate, and peripheral regions while excluding the edge of the culture vessel due to the difficulty of the image due to the viscus effect. These positions were evenly spread in a square–shaped grid to show directionality within a round–shaped culture dish to understand the effect of motion in cell culturing. As the regional area (A_{reg}) covers the margin–less image area (A_{img}), the size of the global area (A_{global}) is the summation of A_{reg} in the 25 sample positions, as given in Eq. (7).

$$A_{global} = \sum_{j=1}^{n_{reg}} A_{reg,j} \tag{7}$$

2.4.5. Defining local and global heterogeneities

Novel indices for spatial heterogeneity were proposed to link different scales of the cell environment (Fig. 2). Local heterogeneity (H_L) is defined as the mean of coefficient of variation (CV) values of local cell densities ($X_{loc,i}$) in each regional area ($A_{reg,j}$) of the global area (A_{global}), as given in Eq. (8). H_L explains single cell behavior by looking at the variation of local cell density (X_{loc}) within each regional area (A_{reg}).

$$\text{For } A_{loc,i} \in A_{reg,j} : \overline{X}_{loc,j} = \frac{1}{n_{loc}} \sum_{i=1}^{n_{loc}} X_{loc,i}$$

$$CV_{loc,j} = \frac{\sqrt{\frac{1}{n_{loc}-1} \sum_{i=1}^{n_{loc}} \left(X_{loc,i} - \overline{X}_{loc,j}\right)^2}}{\overline{X}_{loc,j}} \tag{8}$$

$$\text{For } A_{reg,j} \in A_{global} : \boldsymbol{H_L} = \overline{\boldsymbol{CV}}_{loc,\boldsymbol{j}} = \frac{\boldsymbol{1}}{\boldsymbol{n}_{reg}} \sum_{\boldsymbol{j=1}}^{\boldsymbol{n}_{reg}} \boldsymbol{CV}_{\boldsymbol{loc,j}}$$

Herein, for all local areas ($A_{loc,i}$) within each regional area ($A_{reg,j}$), $\overline{X}_{loc,j}$ is the mean local cell densities ($X_{loc,i}$) in each regional area ($A_{reg,j}$), $CV_{loc,j}$ is the CV of local cell densites ($X_{loc,i}$) in each regional area ($A_{reg,j}$). For all each regional areas ($A_{reg,j}$) within the global area (A_{global}), $\overline{CV}_{loc,j}$ is the mean of local cell density ($X_{loc,i}$) coefficients of variation between regional areas ($A_{reg,j}$).

Global heterogeneity (H_G) is defined as the CV of mean regional cell densities ($X_{reg,n}$) in the global area (A_{global}), as given in Eq. (9). H_G explains the variation between different regions and sub-populations of the total cell culture.

$$\text{For } A_{reg,j} \in A_{global} : \overline{X} = \frac{1}{n_{reg}} \sum_{j=1}^{n_{reg}} \overline{X}_{loc,j}$$

$$\boldsymbol{H_G} = CV_{reg} = \frac{\sqrt{\frac{1}{n_{reg}-1} \sum_{j=1}^{n_{reg}} \left(\overline{X}_{reg,j} - \overline{X}\right)^2}}{\overline{X}} \tag{9}$$

Herein, for all regional areas ($A_{reg,j}$) within the global area (A_{global}), $\overline{X}$ is the mean local cell density ($X_{loc,i}$) in the global area, while CV_{reg} is the CV of mean regional cell densities ($X_{reg,n}$).

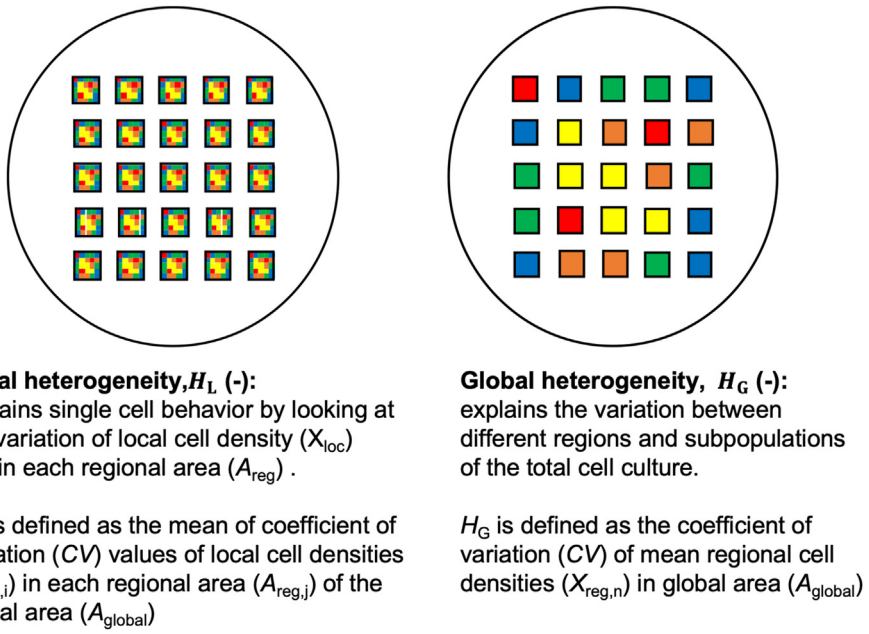

Fig. 2. Definitions of Local and Global heterogeneity. A conceptual diagram illustrating the definitions of local and global spatial heterogeneity within a culture vessel. The circles represent the culture vessels, with each large square indicating a regional area and each small square representing a local area. The colors of the squares denote variations in cell density.

To calculate the spatial heterogeneity indices, a customized image analysis method was used, where raw digital images of stained cell nuclei were used as input, the centroids of cell nuclei were detected, local cell densities were calculated, and a density heatmap was generated (Fig. 3).

3. Results

3.1. Trends of initial cell distribution following cell seeding

Cell distribution was observed after cell seeding according to the conventional method (control), prolongated time of cell seeding suspension (waiting) and vessel tilting during cell seeding operation (tilting). These methods produced different patterns of cell distributions in cell culture vessels (Fig. 4a). Heatmaps of cell local densities showed relatively uniform cell density in the control method of cell seeding, where close color pallets exhibited among the 25 regional areas as well as within each regional area. Cell distributions showed a relatively similar cell density between regional areas of waiting method, while the cell density range within each regional area was considerably diverse. In the tilting method, cell distribution showed a wider variation between regional areas along the direction of vessel tilting, with a lesser variation within each regional area.

This change of patterns was further elucidated by distribution plots (Fig. 4b). In control method, plots followed a normal distribution, relatively overlapping with narrow shapes, suggesting the proximity of means of local density in regional areas forming a unimodal distribution, as well as less divergence from the mean. In elongated waiting time, plots were wider, skewed to lower cell density, and relatively overlapping, suggesting higher variation of cell density within each regional area with the appearance of more local areas expressing high local densities due to cell gathering during the elongated waiting time in a cell seeding suspension, as well as more local areas expressing lower local cell densities due to single cells that did not aggregate in the remaining cell suspension. Additionally, the plots of each regional area were relatively overlapping, suggesting a small variance between regional areas, forming a unimodal distribution. In vessel tilting, the plots showed a narrow distribution, suggesting the proximity of local densities to the mean in each regional area. However, these plots were less overlapping with different peaks with variance between means of local densities in regional areas, forming a multimodal distribution.

Calculations were performed to elucidate the difference in these distribution patterns (Table 1), where the grand mean of local cell density (X_{loc}) in each regional area (A_{reg}) was higher in control and tilting than in the waiting method, 1.95×10^5, 1.86×10^5, and 1.75×10^5 cell/cm^2, respectively, suggesting overall shifting toward a lower mean cell density in tilting and waiting methods. Additionally, the average standard deviation of local cell densities (X_{loc}) in each regional area (A_{reg}) was low in both control and tilting methods, 0.29×10^5 cell/cm^2, and high in the waiting method, 0.41×10^5 cell/cm^2, expressing the wider and skewed distributions in each regional area occurring in the waiting method compared with narrower distributions in control and tilting methods. However, the standard deviation of the mean of local density (X_{loc}) in each regional area, A_{reg}, was higher in tilting and waiting than in the control method, 0.46×10^5, 0.14×10^5, and 0.09×10^5 cell/cm^2, respectively, suggesting less overlapping and less proximity of the means of local density in regional areas forming a multimodal distribution in tilting method, while higher overlapping and unimodal distribution in control and waiting methods. Additionally, mean of maximum frequency in distribution of local cell densities (X_{loc}) among regional areas, A_{reg}, was higher in control and tilting methods, 0.21×10^5, compared with the waiting method, 0.15×10^5, suggesting a narrower distribution with the peaks of each regional area containing a higher frequency of local cell densities (X_{loc}) in control and tilting methods.

The calculations were useful in expressing the shapes and differences between patterns of cell distributions. As a relative measure of variability, the coefficient of variation was used instead of standard deviation for further analysis. Therefore, the mean of coefficient of variation of local cell densities (X_{loc}) in each regional area (A_{reg}) was considered for proposing the local heterogeneity

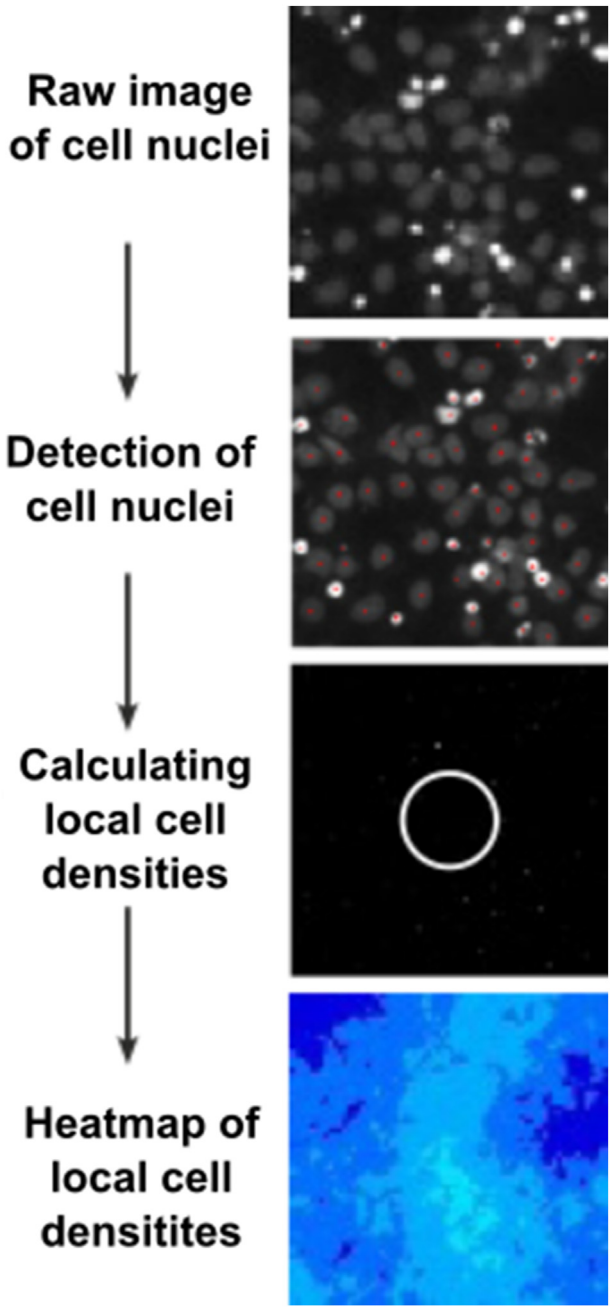

Fig. 3. Calculation of Local Cell Densities. The positions of cells were measured 24 h after seeding to calculate local cell densities. The process involves: (1) obtaining raw images of cell nuclei, (2) detecting cell nuclei, (3) calculating local cell densities, and (4) generating density heatmaps to visualize patterns of spatial heterogeneity.

(H_L), while the coefficient of variation of the mean of local density (X_{loc}) in each regional area, A_{reg}, was considered for the global heterogeneity (H_G) (Fig. 2).

3.2. Effect of cell seeding methods in spatial heterogeneity

Spatial heterogeneity analysis was employed to understand patterns arising from the modified cell seeding technique. Local (H_L) and global heterogeneities (H_G) were assessed across three different seeding methods: control, waiting, and tilting. Eight independent experimental runs were conducted, each comprising three culture dishes (n = 24) (Fig. 5). For comparative analysis, H_L and H_G were graphically plotted against each other, revealing method–dependent clustering of data. The clustering was the highest in the control method, demonstrating the lowest degrees of H_L and H_G. Conversely, the waiting method displayed increased H_L with moderate H_G and less clustering. The tilting method showed a broader spread, higher H_G values, and moderate H_L. The observed clustering patterns provide insight into the impact of the cell seeding technique and the magnitude and variation of cellular heterogeneity.

3.3. Effect of cell seeding on cell fate

To elucidate the consequences of modified cell seeding methods on spatial heterogeneity and cell fate, hiPSC were directed toward a neuroectodermal lineage, which is known to be sensitive to cell density during differentiation. These hiPSC, confirmed to maintain pluripotency via flow cytometry using the octamer–binding transcription factor as a pluripotency marker, were used as the initial stock for differentiation induction. Additionally, these cells exhibited no expression of the paired box protein 6 (PAX6), used here as a biomarker for cells differentiating toward the neuroectodermal lineage, nor of cytokeratin 18 (CK18), indicating differentiation toward an epithelial lineage, used here as a negative control to identify non–target cells.

After seven days of differentiation induction into the neuroectodermal lineage, the cells underwent assessment through double immunostaining for PAX6 and CK18 markers. The resulting cellular expression profiles were representatively categorized within a quadrant plot (Fig. 6a), outlining the subsets of cells expressing neither marker, only one marker, or both markers concurrently. The data primarily revealed three distinct patterns of marker expression among the populations: a majority displayed PAX6 positivity with CK18 negativity (PAX6+/CK18-) as target cells, a substantial fraction exhibited exclusive CK18 positivity and PAX6 negativity (PAX6-/CK18+), and a minority were negative for both markers (PAX6-/CK18-) or dual–positive for both markers (PAX6+/CK18+). These observations hint at a transition from undifferentiated hiPSC (PAX6-/CK18-) toward cells committed to the neuroectodermal lineage (PAX6+/CK18-) as target cells, or toward divergent lineages such as the epithelial lineage (PAX6-/CK18+).

We analyzed the impact of different cell seeding methods on variability in cell commitment toward the neuroectodermal lineage across 24 independent cultures (Fig. 6b). The Shapiro-Wilk test confirmed non-normal data distribution, and the Kruskal-Wallis H test showed no statistically significant differences between the control, waiting, and tilting methods. Since statistical tests focus on averages, we further investigated variability using coefficient of variation (CV) analysis and outlier assessment, revealing important differences (Supplementary Table S1). The control method had the lowest variability with a CV of 0.12 (0.06 without outliers), the waiting method had a CV of 0.16 (0.08 without outliers), and the tilting method showed the highest variability with a CV of 0.17 (0.13 without outliers). In the control method, two outliers had higher PAX6+/CK18- expression, while all outliers in the waiting and tilting methods showed lower expression. Non-target cell populations, including PAX6+/CK18+ and PAX6-/CK18+, showed stable CVs across all methods, but the PAX6-/CK18- population exhibited the highest variability in the tilting method (CV = 0.77). Overall, the control method had the least variability, while the tilting method showed the greatest variability in cell fate. Although no statistically significant differences were observed, the CV analysis considering outliers provided valuable insights into the differentiation process, consistent with previous studies using this approach to assess process stability in cell manufacturing [16].

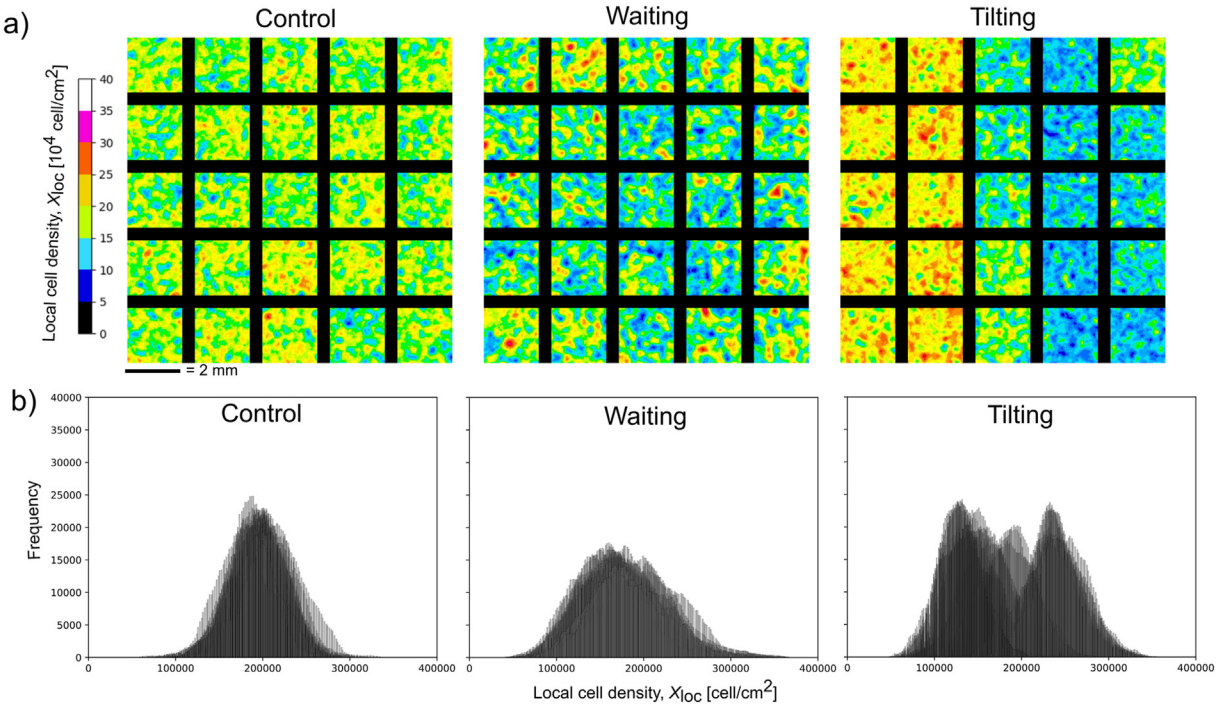

Fig. 4. Effect of Cell Seeding Methods on Cell Distribution. (a) Density heatmaps showing local cell densities for representative cases across different cell seeding methods (control, waiting, and tilting). Cell positions were captured 24 h after seeding, across 25 regional areas within each culture vessel. (b) Histograms representing local cell densities 24 h after seeding for each of the 25 regional areas in the representative seeding methods. Each histogram bin width is 2000 cells/cm^2.

Table 1
Descriptive summary statistic of local cell densities histograms at the 24 h across 25 regional areas in representative cases of cell seeding conditions.

Parameter	Unit	Control	Waiting	Tilting
Grand mean of local cell densities, X_{loc}, in each regional area, A_{reg}	[10^5 cells/cm^2]	1.95	1.75	1.86
Mean of standard deviation of local cell densities, X_{loc}, in each regional area, A_{reg}	[10^5 cells/cm^2]	0.29	0.41	0.29
Standard deviation of mean of local cell densities, X_{loc}, in each regional area, A_{reg}	[10^5 cells/cm^2]	0.09	0.14	0.46
Mean of maximum frequency in distribution of local cell densities, X_{loc}, among regional areas, A_{reg}	[10^5]	0.21	0.15	0.21

Moreover, the proportion of non−target cell groups indicated low percentages of PAX6+/CK18+, PAX6-/CK18+, and PAX6-/CK18- across all seeding methods. The control method showed a lower variability and a trend toward lower percentages of the three non−target categories. While the waiting and tilting cultures also had a low PAX6-/CK18+ percentage, there was a higher spread and skewness toward a higher PAX6-/CK18+ percentage than the control. These observations suggest that while a small fraction of the cell population across all methods diverged and differentiated toward non−target epithelial lineages, the control methods showed slightly fewer such cells. Similarly, this broader distribution was visible in waiting culture PAX6-/CK18- percentages and the highest in tilting cultures, with skewness toward a lower PAX6-/CK18- percentage. This suggests that a moderate proportion of the cell population remained undifferentiated in the tilting method, with a lesser extent in the waiting method and the least in the control methods.

There were no substantial disparities in the PAX6+/CK18+ percentages across the method, indicating that a comparable proportion of cells underwent dual staining for both markers. This identified them as non−target cells owing to their potential commitment to lineages expressing both markers. It might be interesting to investigate whether these cells commit to an intermediate or alternative lineage.

4. Discussion

The successful development of cell culture systems relies on a thorough understanding of cellular behavior and how it is influenced by different culture processes. A critical step in this process is cell seeding into the culture vessel, where initial conditions, such as seeding density and cell distribution within the vessel, are believed to affect cell fate [6,7,12]. Even with a target cell density, seeding can result in various distribution patterns due to initial seeding density and the scale of cell culturing, leading to varying local densities and unpredictable cellular behavior. Several parameters in the seeding process influence cell distribution, including the duration of culture movements, the interval between subsequent operations, preparation of the target seeding suspension volume, effective cell dissociation, ensuring a single−cell suspension, and external forces applied to culture vessels.

Previous studies have indicated that reducing the initial seeding density positively affects cultivation and enhances global heterogeneity [14,17–20]. The proliferation of anchorage−dependent mammalian cells can be described by stochastic models, such as cellular automata [21,22], where simulation results using these models have predicted the impact of heterogeneity in the spatial distribution of seeded cells on growth rates [23–26]. This study investigated cell seeding by analyzing cell positioning within the culture environment, from individual cell locations to the entire

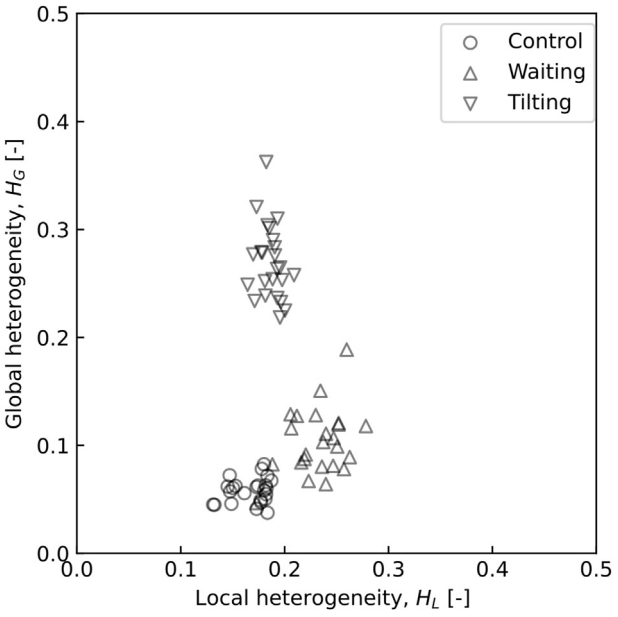

Fig. 5. Effect of Cell Seeding Methods on Spatial Heterogeneity. Scatterplot showing the local heterogeneity (H_L) and global heterogeneity (H_G) for three cell seeding methods (control, waiting, and tilting; $n = 24$). Cell positions were captured 24 h after seeding, from 25 regional areas within each culture vessel.

culture area. We proposed a method that examines the heterogeneity of cell distribution. Two primary indices were proposed: local heterogeneity (H_L), which considers density variations at a cellular locality, and global heterogeneity (H_G), which considers the whole culture area. Factors related to preparing a single–cell seeding suspension influence local heterogeneity, whereas procedures such as determining the cell position in the culture vessel and tilting or shaking the vessel affect global heterogeneity.

Current findings indicate that a prolonged waiting period during cell seeding suspension leads to an increased local heterogeneity due to cell clustering. Furthermore, tilting the culture vessel after inoculation produces greater global heterogeneity. With high–density seeding, we observed varied cellular environments. In regions of low density, cells from single–cell suspensions attached independently to the substrate–coated vessel, allowing ample space for growth and colony formation. These cells typically exhibited a more expansive structure with stronger connections to the substrate than other cells. On the contrary, in high–density areas, cells attached to the substrate and connected with adjacent cells owing to space constraints, resulting in a densely packed cell culture and a multilayered cell sheet structure marked by robust cell–to–cell connections. If cell aggregation occurred during seeding, the behavior mimicked that of adherent cells in high–density areas, forming larger multilayered structures. These aggregated cells may attach to existing adherent cells or remain unattached, expanding and potentially being lost during medium changes. Ultimately, these findings highlight the diverse cell structures that can emerge, ranging from loose and expansive to

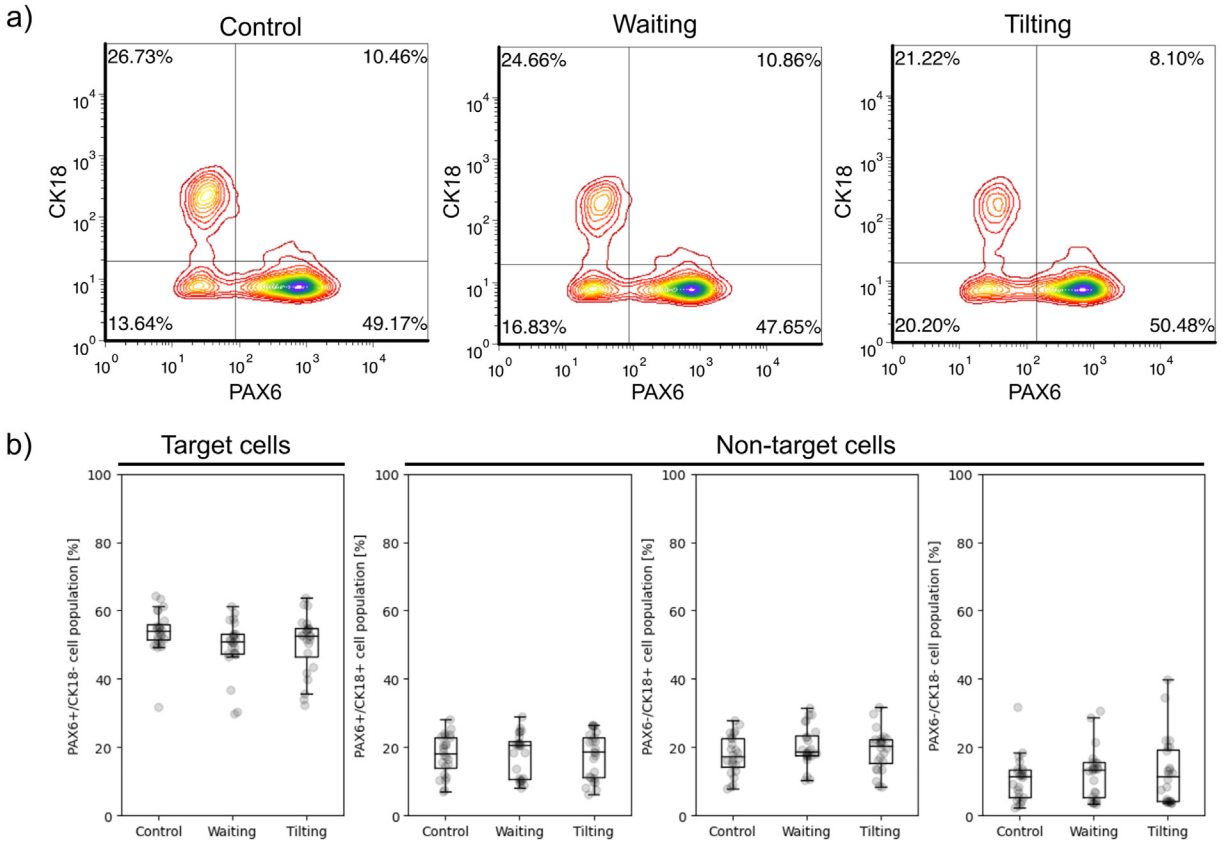

Fig. 6. Effect of Cell Seeding Methods on hiPSC-Neuroectodermal Differentiation. (a) Quadrant plots from flow cytometric analysis showing the expression of PAX6 and CK18 markers under different cell seeding methods (control, waiting, and tilting). (b) Boxplots showing the percentage of cells expressing PAX6 and CK18 at day 7 of neuroectoderm differentiation. The left plot showed cell population with target cell expression of PAX6+/CK18-, followed by cell population with non-target cell expression of PAX6+/CK18+, PAX6-/CK18+, and PAX6-/CK18- respectively. Data were obtained from flow cytometric analysis across 24 independent experiments. For each box, the central bar represents the median, the edges indicate the 25th and 75th percentiles, and the whiskers extend to the most extreme data points (excluding outliers).

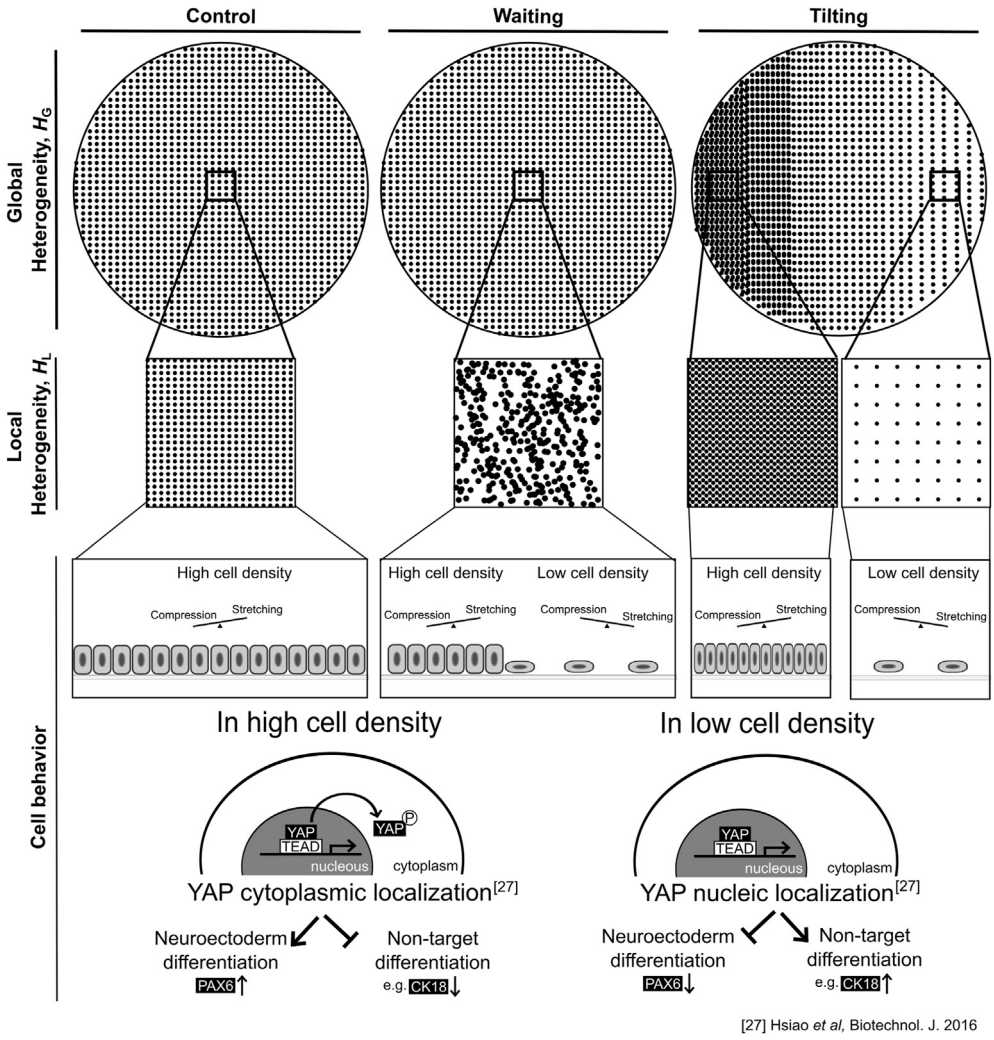

Fig. 7. Role of Spatial Heterogeneity in hiPSC–Neuroectodermal Differentiation. In the current hypothesis, local cell densities vary across the culture vessel depending on the cell seeding methods. In areas with high cell density, a compact cell structure is thought to experience higher cell compression, resulting in YAP cytoplasmic localization. This leads to the inactivation of the YAP/TAZ signaling pathway and induces hiPSC–neuroectodermal differentiation. In contrast, in areas with low cell density, a loose cell structure is thought to experience higher stretching, resulting in YAP nuclear localization. This leads to the activation of the YAP/TAZ signaling pathway and inhibits hiPSC–neuroectodermal differentiation.

dense and compact formations, underscoring the complexity and importance of understanding cell seeding dynamics.

The differentiation of pluripotent stem cells into specific lineages is influenced by cell density. For instance, higher cell density is conducive to differentiation into the neuroectoderm lineage. Cells react to external mechanical signals, such as shear stress and stiffness, which can influence their structure and function and initiate downstream mechanobiological responses [27–29]. These responses are believed to regulate cell homeostasis, preserving self–renewal and pluripotency or guiding differentiation into specific lineages [28,30–32]. In addition, Hsiao *et. al* [28]. describe that in high–density regions of cell culture, there is inactivation of the Yes–associated protein (YAP) and transcriptional coactivator with PDZ–binding motif pathways, leading to differentiation toward the neuroectoderm lineage through cytoplasmic translocation. In contrast, in lower–density regions, nuclear translocation of YAP activates the YAP/transcriptional coactivator with the PDZ–binding motif pathway, which inhibits neuroectoderm differentiation and redirects it toward other lineages, including the epidermal cell lineage, suggesting similar results in our study.

Analyzing spatial heterogeneity offers insights into the operational parameters or cell traits that influence the degree and scope of spatial variations, serving as a tool to refine the cell culture process. Our goal was to understand and regulate the impact of cell seeding operations by examining spatial variations and determining cell outcomes (Fig. 7). This scrutiny can be incorporated into process stability evaluations, helping assess consistency across and within batches. It can also be useful in quality control, predicting the results of the cell manufacturing process and refining cell culture operations. To reduce undesirable spatial patterns, one can consider mechanizing cell culture to curb process inconsistencies and employ optimized operational parameters. Another approach is to directly influence cell behavior, reorganizing cells to achieve the preferred density and distribution.

5. Conclusion

Quality control indices were proposed for hiPSC cultures, where spatial heterogeneity following high–density cell seeding is analyzed. Global heterogeneity (H_G) was shown to be affected by vessel tilting, while local heterogeneity (H_L) was influenced by a

prolonged waiting period during cell suspension. Both changes in spatial heterogeneity were found to result in a lower yield of target neuroectodermal cells compared with control operations. Understanding spatial heterogeneity in the early stages detects errors in cell culture motion and predicts cell fate in later stages of cell culture.

Declaration of competing interest

The authors declare that they have no known competing financial interests or personal relationships that could have appeared to influence the work reported in this paper.

Acknowledgments

This work was supported by Project Focused on Developing Key Evaluation Technology: Development of Platform Technology for Drug Discovery through the Application of Regenerative Medicine from the Japan Agency for Medical Research and Development (AMED) under grant number JP19be0604001 and the Project Focused on Establishment of QbD–based control strategy and advanced core ecosystem in cell manufacturing from AMED under grant number JP20be0704001.

Appendix A. Supplementary data

Supplementary data to this article can be found online at https://doi.org/10.1016/j.reth.2024.10.006.

References

[1] Shi Y, Inoue H, Wu JC, Yamanaka S. Induced pluripotent stem cell technology: a decade of progress. Nat Rev Drug Discov 2017. https://doi.org/10.1038/nrd.2016.245.
[2] Kino-oka M, Mizutani M, Medcalf N. Cell manufacturability. Cell Gene Ther Insights 2019. https://doi.org/10.18609/cgti.2019.140.
[3] Horiguchi I, Kino-oka M. Current developments in the stable production of human induced pluripotent stem cells. Engineering 2021. https://doi.org/10.1016/j.eng.2021.01.001.
[4] Thanuthanakhun N, Kim MH, Kino-oka M. Cell behavioral dynamics as a cue in optimizing culture stabilization in the bioprocessing of pluripotent stem cells. Bioengineering 2022. https://doi.org/10.3390/bioengineering9110669.
[5] Ratcliffe E, Thomas RJ, Williams DJ. Current understanding and challenges in bioprocessing of stem cell-based therapies for regenerative medicine. Br Med Bull 2011. https://doi.org/10.1093/bmb/ldr037.
[6] Reynolds RM, Holzmann Rasmussen C, Hansson M, Dufva M, Riehle MO, Gadegaard N. Controlling fluid flow to improve cell seeding uniformity. PLoS One 2018. https://doi.org/10.1371/journal.pone.0207211.
[7] Berent ZT, Wagoner Johnson AJ. Cell seeding simulation on micropatterned islands shows cell density depends on area to perimeter ratio, not on island size or shape. Acta Biomater 2020. https://doi.org/10.1016/j.actbio.2020.02.035.
[8] Kam KM, Zeng L, Zhou Q, Tran R, Yang J. On assessing spatial uniformity of particle distributions in quality control of manufacturing processes. J Manuf Syst 2013. https://doi.org/10.1016/j.jmsy.2012.07.018.
[9] Jaccard N, Griffin LD, Keser A, Macown RJ, Super A, Veraitch FS, Szita N. Automated method for the rapid and precise estimation of adherent cell culture characteristics from phase contrast microscopy images. Biotechnol Bioeng 2014. https://doi.org/10.1002/bit.25115.
[10] Kato Y, Kim KH, Kino-oka M. Comparison of growth kinetics between static and dynamic cultures of human induced pluripotent stem cells. J Biosci Bioeng 2018. https://doi.org/10.1016/j.jbiosc.2018.01.002.
[11] Kepp O, Galluzzi L, Lipinski M, Yuan J, Kroemer G. Cell death assays for drug discovery. Nat Rev Drug Discov 2011. https://doi.org/10.1038/nrd3373.
[12] Gage BK, Webber TD, Kieffer TJ. Initial cell seeding density influences pancreatic endocrine development during in vitro differentiation of human embryonic stem cells. PLoS One 2013. https://doi.org/10.1371/journal.pone.0082076.
[13] Watt FM. Effect of seeding density on stability of the differentiated phenotype of pig articular chondrocytes in culture. J Cell Sci 1988. https://doi.org/10.1242/jcs.89.3.373.
[14] Fossett E, Khan WS. Optimising human mesenchymal stem cell numbers for clinical application: a literature review. Stem Cell Int 2012. https://doi.org/10.1155/2012/465259.
[15] Takahashi M, Okamoto S, Sakai N. Method of producing human retinal pigment epithelial cells. Patent No. JP2013212345A.
[16] Nair A, Horiguchi I, Fukumori K, Kino-oka M. Development of instability analysis for the filling process of human-induced pluripotent stem cell products. Biochemical Eng 2022. https://doi.org/10.1016/j.bej.2022.108506.
[17] Scholz BX, Hayashi Y, Udugama IA, Kino-oka M, Sugiyama H. A CFD model-based design of seeding processes for two-dimensional mesenchymal stem cell cultivation. Comput Chem Eng 2023. https://doi.org/10.1016/j.compchemeng.2023.108157.
[18] Hirono K, Udugama IA, Hayashi Y, Kino-oka M, Sugiyama H. A dynamic and probabilistic design space determination method for mesenchymal stem cell cultivation processes. Ind Eng Chem Res 2022. https://doi.org/10.1021/acs.iecr.2c00374.
[19] Pereira AR, Lipphaus A, Ergin M, Salehi S, Gehweiler D, Rudert M, Hansmann J, Herrmann M. Modeling of the human bone environment: mechanical stimuli guide mesenchymal stem cell–extracellular matrix interactions. Materials 2021. https://doi.org/10.3390/ma14164431.
[20] Zhang Z, Du J, Wei Z, Wang Z, Zhang H, Li M, Tang Y. Numerical simulation of dynamic seeding of mesenchymal stem cells in pore structure. Comput Math Appl 2020. https://doi.org/10.1016/j.camwa.2018.01.027.
[21] Lim JHR, Davies GA. A stochastic model to simulate the growth of anchorage dependent cells on flat surface. Biotechnol Bioeng 1990. https://doi.org/10.1002/bit.260360602.
[22] Zygourakis K, Bizios R, Markenscoff P. Proliferation of anchorage-dependent contact-inhibited cells: I. Development of theoretical models based on cellular automata. Biotechnol Bioeng 1991. https://doi.org/10.1002/bit.260380504.
[23] Zygourakis K, Markenscoff P, Bizios R. Proliferation of anchorage-dependent contact-inhibited cells. II: experimental results and validation of the theoretical models. Biotechnol Bioeng 1991. https://doi.org/10.1002/bit.260380505.
[24] Ruaan RC, Tsai GJ, Tsao GT. Monitoring and modeling density-dependent growth of anchorage-dependent cells. Biotechnol Bioeng 1993. https://doi.org/10.1002/bit.260410313.
[25] Lee Y, Kouvroukoglou S, McIntire LV, Zygourakis K. A cellular automaton model for the proliferation of migrating contact-inhibited cells. Biophysics 1995. https://doi.org/10.1016/S0006-3495(95)79996-9.
[26] Kagawa Y, Kino-oka M. An *in silico* prediction tool for the expansion culture of human skeletal muscle myoblasts. R Soc Open Sci 2016. https://doi.org/10.1098/rsos.160500.
[27] Barzegari A, Gueguen V, Omidi Y, Ostadrahimi A, Nouri M, Pavon-Djavid G. The role of Hippo signaling pathway and mechanotransduction in tuning embryoid body formation and differentiation. J Cell Physiol 2020. https://doi.org/10.1002/jcp.29455.
[28] Hsiao C, Lampe M, Nillasithanukroh S, Han W, Lian X, Palecek SP. Human pluripotent stem cell culture density modulates YAP signaling. Biotechnol J 2016. https://doi.org/10.1002/biot.201500374.
[29] Kim MH, Kino-oka M. Mechanobiological conceptual framework for assessing stem cell bioprocess effectiveness. Biotechnol Bioeng 2021. https://doi.org/10.1002/bit.27929.
[30] Pocaterra A, Romani P, Dupont S. YAP/TAZ functions and their regulation at a glance. J Cell Sci 2020. https://doi.org/10.1242/jcs.230425.
[31] Shibata S, et al. Cell-type-specific adhesiveness and proliferation propensity on laminin isoforms enable purification of iPSC-derived corneal epithelium. Stem Cell Rep 2020. https://doi.org/10.1016/j.stemcr.2020.02.008.
[32] Kim MH, Thanuthanakhun N, Fujimoto S, Kino-oka M. Effect of initial seeding density on cell behavior-driven epigenetic memory and preferential lineage differentiation of human iPSCs. Stem Cell Res 2021. https://doi.org/10.1016/j.scr.2021.102534.